

# **Probability of secondary muons in $Z \rightarrow 2$ muon signal in search for the Higgs boson**

**Chris Farrell**

**University of Florida**

## **Abstract**

The Higgs boson is hoped to be discovered at the Large Hadron Collider (LHC) when it begins running in 2008. The most promising channel for its discovery is the decay path  $\text{Higgs} \rightarrow 2 Z \text{ bosons} \rightarrow 4 \text{ muons}$ . The leading order backgrounds for this signal have been well studied but insufficient knowledge exists regarding the total influence of the lower order backgrounds. The project seeks to determine the probability of finding four muons in a  $Z \rightarrow 2\text{muons} + \text{jets}$  event. Furthermore, the author minimizes this probability through variable cuts and classifies the source of the muons for use in future studies. The probability for fake muons can be reduced to 0.205% while still keeping 94.58% of the Z muon signal. No four muon invariant masses can be formed after the completion of variable cuts, so larger statistics are required for future studies.

## **Introduction**

The Higgs boson is a theoretical particle necessary for the Standard Model to work and it is hoped to be discovered at the LHC at the European Organization for Nuclear Research (CERN) when it begins running in 2008. The Standard Model prohibits particles from having mass; instead, it is theorized that mass results from particles coupling with the Higgs field [1]. The Higgs boson is the last prediction of the Standard Model yet to be discovered.

Scientists have searched for the Higgs boson previously at CERN and other facilities but it has yet to be discovered. The LHC will provide 14 TeV of energy,

which is enough to either discover the Higgs boson or prove that it does not exist [2]. If the Higgs boson does not exist, LHC may provide clues as to the new physics responsible for the masses of particles.

The LHC has two detectors collecting data, the Compact Muon Solenoid (CMS) and ATLAS. The two detectors are meant to provide redundancy and cross-checking of data. CMS is built in cylindrical layers with all layers except for the muon chambers built inside a 4 T solenoid [3]. The innermost layers of LHC are silicon detectors used to identify the momentum of all charged particle tracks with a precision of 1%. Surrounding these track detectors are calorimeters that measure the energy of particles in all directions. Only muons and neutrinos have a high probability to pass through the calorimeter. The neutrino interacts too weakly to ever be detected but the muons are identified in muon chambers located outside the solenoid.

The CMS detector will search for the Higgs boson over its range of possible masses between 114 GeV and 1 TeV as well as over numerous different decay channels. The “golden decay” of the Higgs boson is  $\text{Higgs} \rightarrow 2 \text{ Z bosons} \rightarrow 4 \text{ muons}$ . The background of this four-muon signal has three main sources, all of which have been reasonably well simulated. The first is  $2 \text{ Z bosons} \rightarrow 4 \text{ muons}$  without Higgs involvement. This background is irreducible because of its close relationship with the Higgs signal. The second background is  $2 \text{ top quarks} \rightarrow 2 \text{ W bosons} + 2 \text{ bottom quarks} \rightarrow 4 \text{ muons}$ . The third main background is  $\text{a Z boson} + 2 \text{ bottom quarks} \rightarrow 4 \text{ muons}$ . The last two backgrounds create muons in jets of hadronic (quark constituent) particles. Jets occur because quarks can not exist alone in nature and must fragment

into a hadronic particle. This fragmentation creates a clustering of particles around the muon that is absent in muons born from a Z boson.

The simulation of  $Z \rightarrow 2$  muon events including secondary muons is much more difficult. Secondary muons are all muons except those from a Z boson, including real muons created from particles colliding into the detector and fake muons reconstructed from random hits in detector. Whether this background creates four muons at a rate significant in comparison to the 2 Z background is unknown at this time. The cross section for  $Z \rightarrow 2$  muon production is large, so even a small rate may be troublesome. This paper seeks to find this rate and to create variable cuts to place on muons in order to minimize the 4-muon probability while maintaining a high efficiency to keep Z boson muons. Classifying the source of the muons will provide direction for future studies. An important goal of the paper is to find whether the probability to get two muons equals the probability of getting one muon squared.

This paper uses simulations in order to devise analysis techniques that can then be used once experimental data become available. The simulations are restricted to collision events that produce a Z boson and jets.

### **Data Samples Used**

The data sample used in this study was created by Monte Carlo simulation and contains three different layers of data. The first layer corresponds to HEP (High Energy Physics) event muons. These muons are created in the initial collision of the protons in the collider. The second layer is GEANT level muons, which contain all HEP layer muons as well as muons from long-lived particle decays and muons created by the physical interaction with the detector. The third layer is Global Muon

Reconstruction (GMR) information available in real data. The calorimeter isolation of these GMR muons is also provided.

## Identifying $Z \rightarrow 2$ muon Events

I only studied events where I believed a Z boson had decayed into two muons. I identified these events by calculating the invariant mass of all oppositely charged muon pairs in an event by Eq. (1) and kept the di-muon pair closest to the mass of the Z boson.

$$M = \sqrt{((\sum E)^2 - (\sum \vec{p})^2)} \quad (1)$$

The energy of the muon is taken to be the magnitude of its momentum with its mass negligible. Figure 1 shows the distribution of HEP level di-muon invariant masses.

The graph has a large peak at the mass of the Z boson. I selected events having a di-muon invariant mass within 10 GeV/c<sup>2</sup> of the Z boson and henceforth will call these on-shell Z events. This width is chosen to capture all of the events creating the peak in the graph.

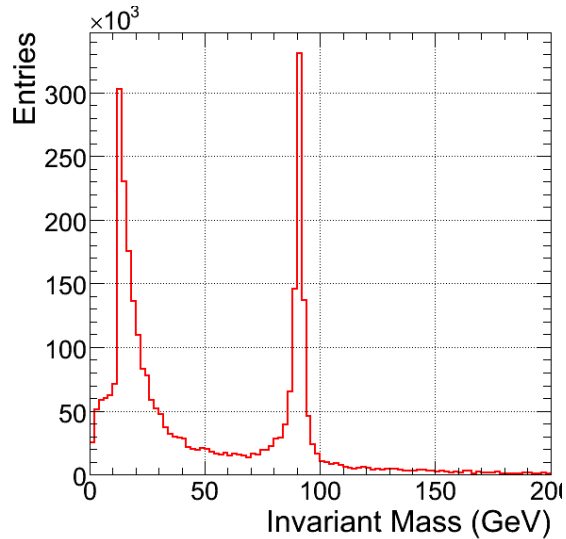


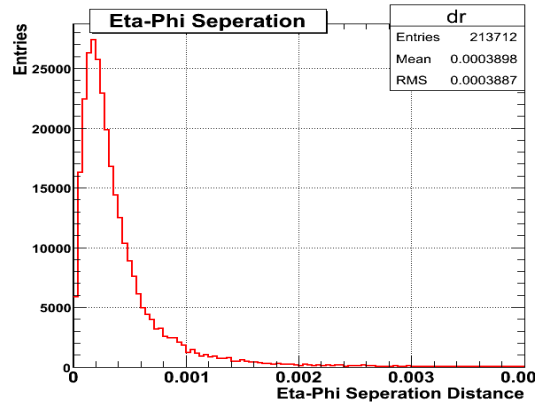
Figure 1 Mass of di-muon pairs at HEP level

## Matching GMR and HEP Z-muons

To identify the source of muons, I had to find a way to match GMR-level and HEP-level muons. This matching is only done for Z-HEP muons in on-shell Z events.

I first tried to do this match using the metric  $\Delta r = \sqrt{(\Delta\eta)^2 + (\Delta\Phi)^2}$  for Z boson muons where  $\Phi$  is the azimuthal angle and  $\eta$  is defined as  $-\ln(\tan(\Theta/2))$ .  $\Theta$  is the polar angle measured in relation to the beam direction. I matched the muons by looping over all GMR and HEP muons, finding the same charged pair with the minimum separation in  $\Delta r$ , removing these muons, and looping over the muons again until I ran out of either GMR or HEP muons. Figure 2 shows the separation distance of HEP muons coming from the Z boson.

**Figure 2 Eta-Phi Separation of Z muons**



This matching metric is a little naïve as  $\eta$  and  $\Phi$  separation are not on exactly the same scale and can depend on  $\eta$ . To correct for these differences I decided to use the elliptical metric in Eq. 2. I found the sigmas, standard deviations,

in this equation by plotting the  $\Phi$  and  $\eta$  separation of the matched muons in different regions of the absolute value of the HEP muon's  $\eta$ . I then fit these distributions to a

$$\Delta r = \sqrt{\left(\frac{\Delta\eta}{\sigma_{\eta}(\eta)}\right)^2 + \left(\frac{\Delta\phi}{\sigma_{\phi}(\eta)}\right)^2} \quad (2)$$

Gaussian distribution and recorded their sigmas. These sigmas were plotted and then fitted to a polynomial. These fits give Eqs. 3 and 4 for  $\eta$  and  $\Phi$  sigma respectively.

$$\sigma_{\eta} = 0.0003371 - 6.552 \cdot 10^{-5} \cdot \eta^2 + 1.445 \cdot 10^{-5} \cdot \eta^4 \quad (3)$$

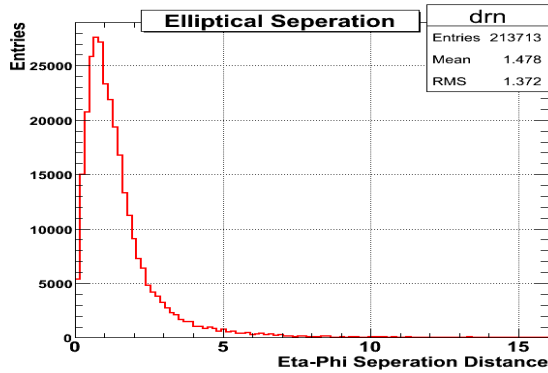
$$\sigma_{\phi} = 0.0001543 + 1.007 \cdot 10^{-5} \cdot \eta^2 + 3.998 \cdot 10^{-6} \cdot \eta^4 \quad (4)$$

Figure 3 shows the new distribution of separation distances between GMR and HEP muons. To determine which matching method is superior, I graphed the efficiency to match muons vs. the probability of a HEP muon matching to more than

one track for various cuts on separation distances. These extra tracks are roughly randomly distributed throughout the detector and thus can provide a quantitative way to

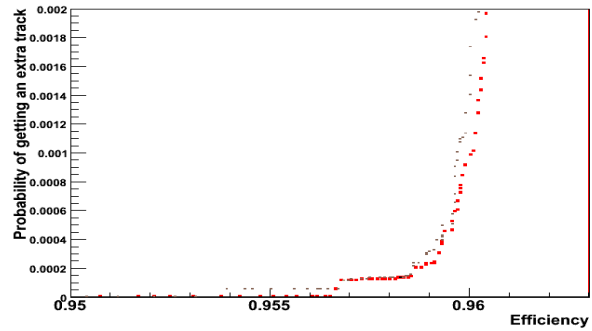
**Figure 3**

**Elliptical Separation Distance**



**Figure 4**

**Efficiency vs. Probability to get Extra Track Comparison**



compare the physical size of the two distances. The efficiency is defined as the number of matches with a separation distance less than the cut divided by the total number of Z-HEP muons. Figure 4 shows this graph with the brown dots corresponding to the regular metric and the red dots to the normalized metric. The normalized metric finds fewer extra tracks at the same Z-muon efficiency, proving it is superior.

### **Matching non-Z HEP and GMR muons**

Next I matched non-Z HEP muons in on shell Z events with GMR muons. I decided to match them separately from the muons above because in general they will have less momentum and thus will scatter more. The matching was done as described above, except because I had fewer statistics, I was unable to split the  $\eta$  and  $\Phi$  separations into beams and had to use them as constant with Eta. Figure 5 shows the distribution for  $\eta$  separation and Figure 6 shows the  $\Phi$  separation. The sigmas for  $\eta$  and  $\Phi$  are 0.000625 and 0.0004357, respectively. Figure 7 shows the efficiency to

reconstruct these muons vs. elliptical cut. I considered any matches with a separation less than 13 a true match.

**Figure 5 Eta Separation**

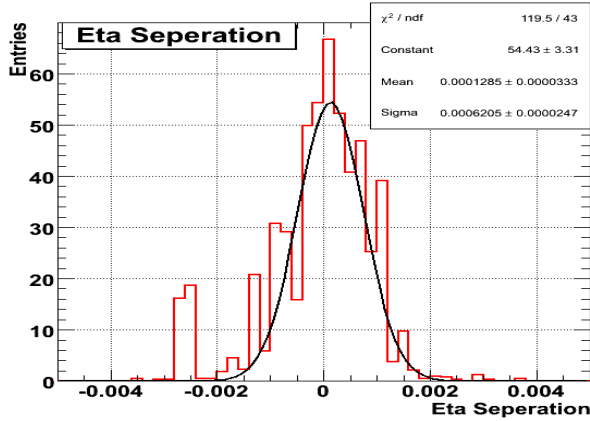


**Figure 6 Phi Separation**

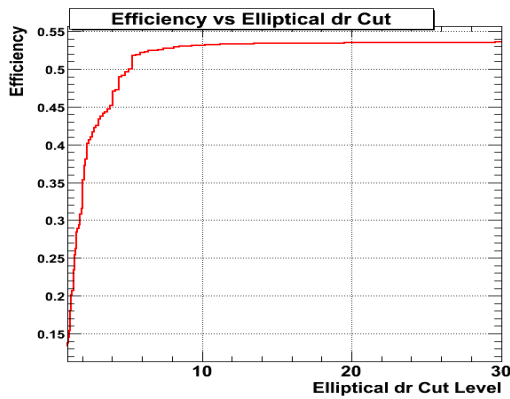
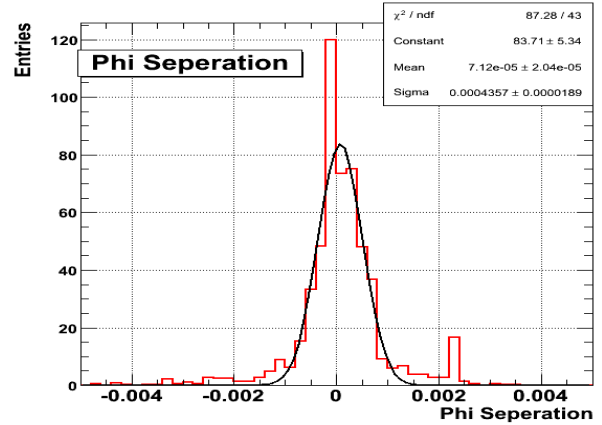


**Figure 7**

**Efficiency vs. Elliptical Cut Distance**

## Matching GMR and GEANT muons

The last matching I need to do is between GEANT muons and GMR muons, which can not be matched to any HEP level muon. This was done by finding on-shell Z events at the GMR level, and matching the GMR muons to HEP muons using the criteria described in the previous section. Once this was done, I attempted to match all the GMR muons to GEANT-level muons. I then only looked at those matches

containing GMR muons not matched to a HEP muon and not used to create the Z muon.

**Figure 8 Eta Separation**

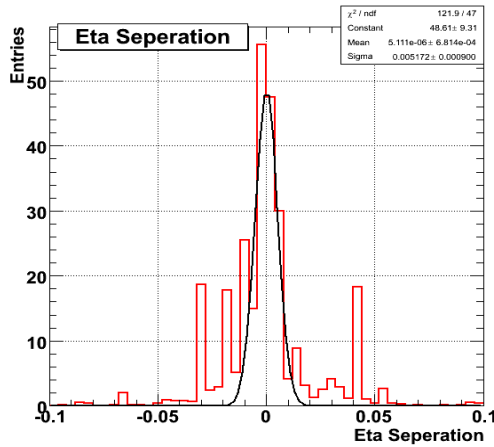
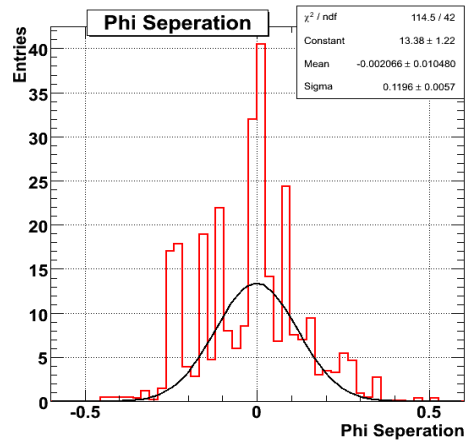


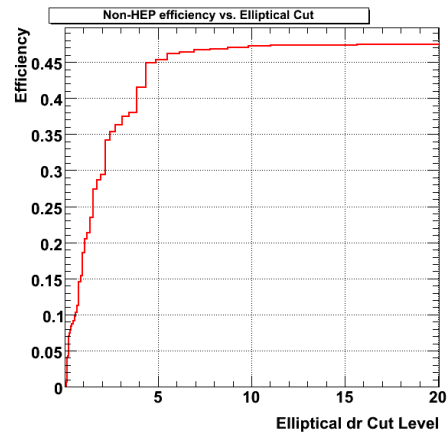
**Figure 9 Phi Separation**



The separation distance is normalized like the non-Z HEP muons above and gave sigmas for  $\eta$  and  $\Phi$  of 0.005172 and 0.1196, respectively, as Figures 8 and 9 show.

Figure 10 shows the efficiency to match these muons as a function of the elliptical cut level. The efficiency in this case was defined as the number of GMR-GEANT muons divided by the number of previously unmatched GMR muons. I placed the cut on these muons at 11 where the graph has hit a plateau.

**Figure 10 Efficiency vs. Elliptical Cut**



## Classifying Secondary Muons

For the purposes of this study I called GMR muons coming from the Z boson “primary muons” and all other GMR muons “secondary muons”. Only on-shell Z events were used and the primary muons were found by looking at the two muons used to make this mass.

The secondary muons were split into four categories based on the matching criteria detailed above. The first category is HEP-level muon and the second is GEANT-level muon. The third category is for ghosts caused by the reconstruction software reconstructing a muon more than once. These ghosts will be very tightly correlated in space. Figure 11 shows

the separation distance between GMR muons of the same charge. I decided to call any muons separated by less than 0.8 in both  $\eta$  and  $\Phi$  as a ghost.

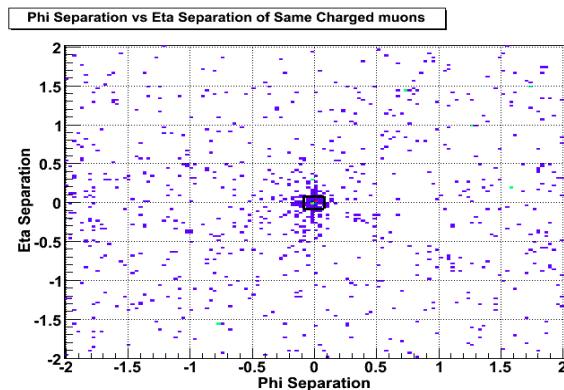
These distances were chosen to

eliminate the central concentration of events in the figure. These ghost muons do show some similarity in momentum but not as closely as separation distance so they are not exact duplicates. I was unable to determine the exact nature of these ghost muons.

Any GMR muons still not classified were called fakes.

The first cut I applied was for Transverse Momentum  $< 7$  and  $|\eta| < 1.1$  or Momentum  $< 13$  and  $|\eta| > 1.1$ . Transverse momentum is momentum perpendicular to the beam direction. This cut was done to move into the plateau region of the reconstruction software’s efficiency curve.

**Figure 11 Eta-Phi Separation of same charged muons**



I next wanted to cut on the calorimeter isolation of the muons. This cut is useful because most of the secondary muons are created in hadronic jets while the primary muons are isolated in space. Figure 12 shows the calorimeter isolation of the different types of muons. I found the optimal cut level by looking at how the efficiency to keep secondary muons and the efficiency to keep primary muons changed with the cut level. Figure 13 shows the efficiency to keep both primary muons vs. the probability to have any secondary muon for various calorimeter isolation cut levels. I placed the cut at a calorimeter isolation of 6.8 which corresponds to an efficiency to keep both primary muons of 98%.

**Figure 12**

**Calorimeter Isolation of muons**

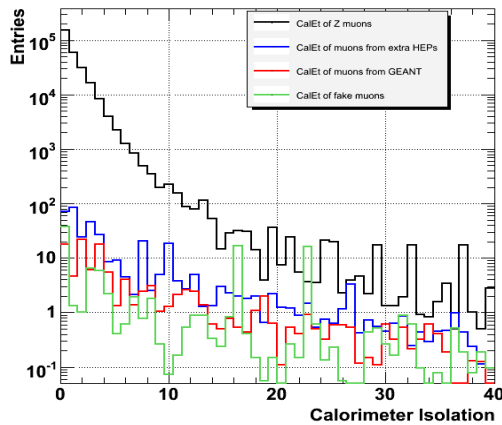
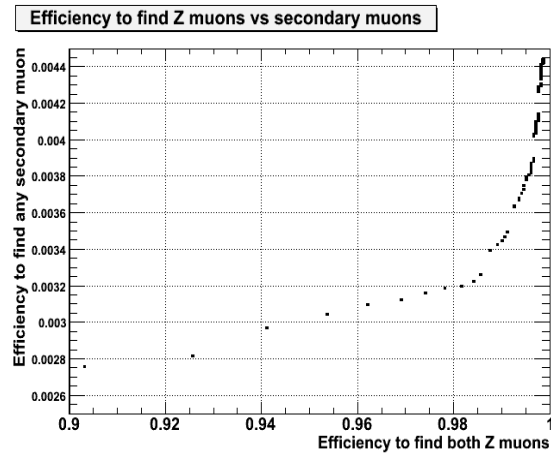


**Figure 13**

**Efficiency comparison at different calorimeter cuts**



Next I imposed a cut on tracker isolation. This cut works for the same reason as the calorimeter cut and because of this duplication has only limited effectiveness.

Figure 14 shows the tracker isolation of the different types of muons. Figure 15 shows

Figure 14

Tracker Isolation of muons

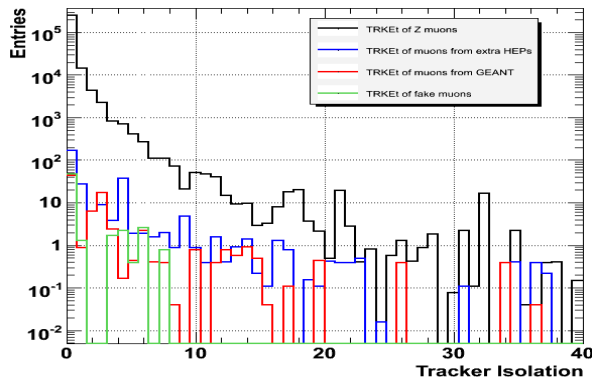
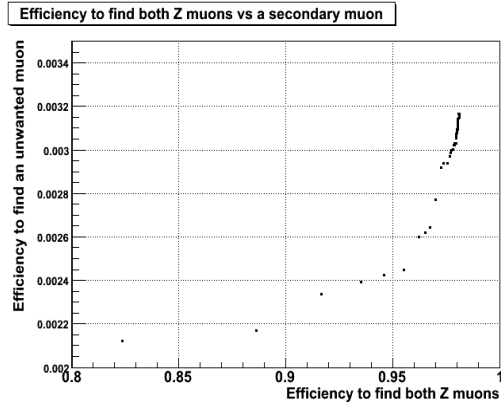


Figure 15

Efficiency comparison at different Tracker cuts



the efficiency to keep both primary muons vs. the probability to have any secondary muons. I decided to place the cut on these muons at 4.4 corresponding to a primary muon efficiency of 97%.

The last cut I made was on number of hits in the muon chambers. This cut was mainly aimed at fake secondary muons reconstructed off random hits. As there are

Figure 16

Number of hits in barrel region

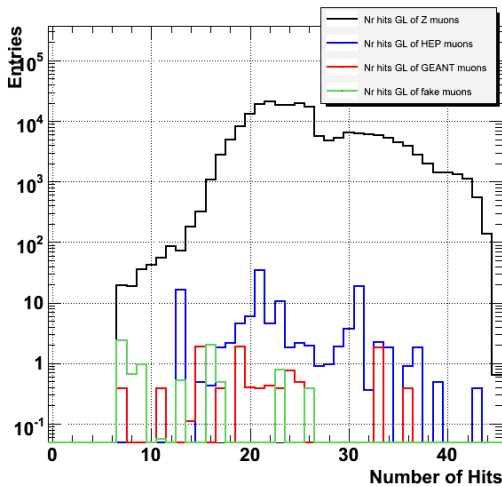
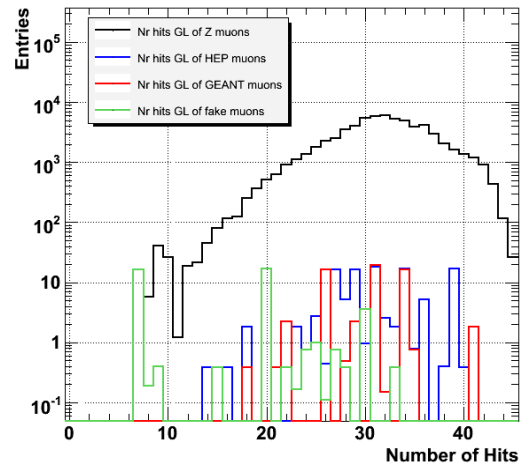
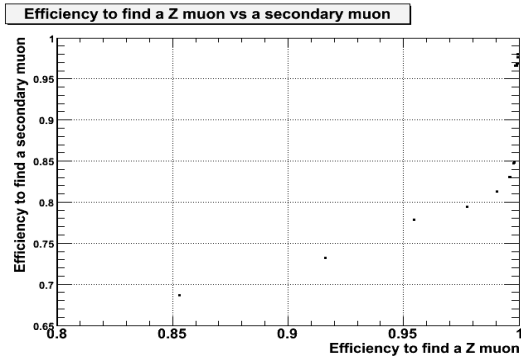


Figure 17

Number of hits in end cap



different layers of detectors in the barrel and end cap region of the detector, a separate cut is needed for the two regions. Figure 16 shows the number of hits in the barrel region for the different muon types while Figure 17 shows the number of hits in the end



**Figure 18 Barrel efficiency comparison**

**For numerous cuts on number of hits**

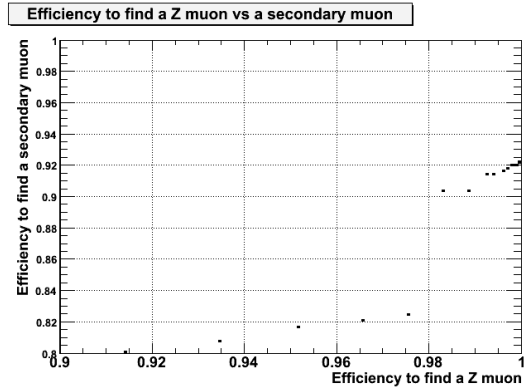


**Figure 19 End cap efficiency comparison**

**for numerous cuts on number of hits**

cap region. Figure 18 shows the efficiency to keep a primary muon vs. a secondary muon in the barrel region while Figure 19 shows the efficiencies for the cap region. I placed the cut in the barrel region at greater than 16 and for the cap region at 20 corresponding to primary efficiency of 99.1% and 97.6%, respectively.

## Discussion

Table 1 shows the probability to find secondary muons after different cuts. The probability drops by a factor 3.75 after all of the cuts, less than what would be hoped for. This may be because the cuts applied were relatively soft in comparison to other studies.

It was hoped that the efficiency to find two secondary muons would equal the probability to find one muon squared. If this was the case, the probability to get two muons could be extrapolated from data once the probability to find one was established. However, these results seem to show this will work only with an accuracy of around 3.

Table 1					
	Primary pair	One secondary	Two secondary	Three secondary	$P_2/(P_1)^2$
Total	1	0.00766519	$1.02428 \cdot 10^{-4}$	$1.92222 \cdot 10^{-6}$	1.7433
Ghost elimination	1	0.00742878	$9.58583 \cdot 10^{-5}$	$1.79883 \cdot 10^{-7}$	1.73698
Pt/P Cut	0.998514	0.00432541	$2.79071 \cdot 10^{-5}$	$3.37083 \cdot 10^{-8}$	1.491627

Calorimeter	0.981807	0.00291371	$1.36807 \cdot 10^{-5}$	0	1.611446
Tracker	0.970156	0.00250203	$1.29041 \cdot 10^{-5}$	0	2.061307
Number of hits	0.945779	0.00204562	$1.28846 \cdot 10^{-5}$	0	3.07908

After all the cuts there were no four-muon events, so I was unable to check if the four-muon mass distribution of this background was larger than the ZZ background. However there will be 1.8 events with two secondary muons at  $0.1 \text{ fb}^{-1}$  compared with 1 ZZ event. These two secondary muons must be of opposite charge and have both Z muons though to create a four muon signal. The statistical uncertainty of these numbers is large as after all the cuts only two events exist with two secondary muons.

Table 2 shows the percentage distribution of the different categories of secondary muons at different cut levels. The ghosts only account for three percent of the total but our lack of understanding about their origin necessitates future study. Fake muons represent 25% of the secondary muons without any cuts but are reduced to 3% after all the cuts. This means an absolute decrease in fake muons of  $3.75 \cdot (25/3) = 30$ , a large amount of suppression. The HEP level is dominant throughout which is good because these are the muons that have been best simulated. The GEANT muons represent nearly a quarter of the muons, and a better simulation of these muons is needed.

	<b>Table 2</b>			
	HEP level	GEANT level	Ghosts	Fakes
Total	47.2048	24.9985	3.23595	24.5604
Ghost elimination	48.7834	25.8345	0	25.3818
Pt/P Cut	62.131	19.3171	0	18.5524
Calorimeter	67.089	19.3552	0	13.5558
Tracker	65.7795	20.0103	0	14.2102
Number of Hits	73.4983	23.3124	0	3.18924

## **Acknowledgments**

I would first like to thank Dr. Andrey Korytov who taught me most of the information in this paper. Without his guidance I would have been stuck at nearly every turn. He has helped teach me not just how to attack this particular project, but also the fundamental ideas in any research endeavor. I would also like to thank Dr. Alexey Drozdetskiy who constantly guided me through physical concepts and technical problems. Nick Kypreos and Matthew Smith were also very helpful in assisting me when I had a bug in my program or a result that did not make sense. The summer has not been just about the research project though, so I would like to thank Dr. Kevin Ingersent for guiding this REU program throughout the summer and for accepting me into the program. Finally I would like to thank the National Science Foundation for its funding of the REU program. The summer experience has grown my understanding of physics and the entire research project, and I appreciate all of the people who have contributed to this experience.

## References

- [1] Alexey Drozdetskiy, Ph. D. thesis, University of Florida, 2007.
- [2] LHC Project, <http://lhc.web.cern.ch/lhc/>,  
[http://lhc-machine-outreach.web.cern.ch/lhc-machine-outreach/lhc in pictures.htm](http://lhc-machine-outreach.web.cern.ch/lhc-machine-outreach/lhc%20in%20pictures.htm).
- [3] CMS Collaboration, <http://cms.cern.ch/>.